

Effect of pumping level on the uniformity of the power and spectrum distributions over the emitting aperture of cw laser diode bars

V.V. Bezotosnyi, V.P. Gordeev, V.A. Oleshchenko

Abstract. Thermal parameters of cw laser diode bars (LDBs) have been studied experimentally and using 3D simulation in order to identify factors limiting their output power and operational life. Using a thermal camera, we have obtained thermal field images of 47-cluster LDBs with an aperture fill factor of 50 %, packaged in a heat spreader of the C–S mount type. Distributions of the output power and emission spectrum of the emitting clusters have been measured by a probing method. The simulation results and experimental data have been analysed, compared and discussed.

Keywords: laser diode bars, cw operation, output power, emission spectrum.

1. Introduction

In previous work [1, 2], a novel laser diode bar (LDB) design with an output power of 60 W in cw mode and up to 300 W in a quasi-cw mode was demonstrated. Thermal conditions of cw LDBs with a standard emitting aperture width of 10 mm were shown to be characterised by significant heat dissipation nonuniformities due to the dissimilar cooling conditions of the central and peripheral clusters [3]. Comparison of peak positions in the emission spectra of the central cluster and outermost peripheral clusters showed good agreement with calculation results for a 19-cluster LDB with a fill factor FF = 50%. It is worth noting that, with increasing output power, especially in continuous mode, it is becoming more and more important not only to raise the efficiency of cooling the active region of the laser chip when extremely large heat fluxes should be dissipated but also to solve the problem of thermal field nonuniformity in LDBs. One example of successful advances in this direction is a recent report [4] that a single cw LDB delivered 880 W of output power, which opens up new possibilities for employing the kilowatt range.

Raising the LDB output power involves the problem of dissipating heat fluxes of extremely high density. One way of resolving this problem is by increasing the cavity length from the standard 2 mm (in commercially available LDBs) to 4 mm and above. The thermal load density can in principle be reduced as well by raising the emitting cluster fill factor of the output aperture from typical 50% to 70% through the optimisation of the emitting cluster width. In addition, raising

the FF allows the optical load density on the output mirror of the LDB to be reduced. Our calculation results [5] indicate that increasing the cavity length at a constant thermal load reduces not only the heat flux density being dissipated but also the temperature difference along the length of the cavity and the temperature of the input mirror. This improves the output parameters and reliability of the bar. At the same time, raising the FF increases the threshold current of the LDB and aggravates the problem of mutual thermal effect of the emitting clusters. Because of this, in constructing a model for LDBs, one should take into account all their key parameters, including the threshold current, the slope of the light–current ($L-I$) characteristic, total efficiency, thermal and series resistances, and their dependences on temperature and thermoelastic stress.

In this paper, which presents one step in constructing such a model, major attention is paid to a more rigorous experimental verification of previous results [3], in particular, by examining distributions of the power and emission spectra of individual clusters, and to direct verification of whether the experimental data are consistent with 3D simulation results. The calculation results and experimental data are of interest by themselves and are important in designing systems for wavelength beam combining of LDBs and 2D laser arrays for direct laser processing of materials [6, 7]. The issues under consideration have been addressed in a considerable number of publications, including Refs [8, 9].

2. Simulation procedure and calculation results

In this study, thermal processes were simulated by the finite element method in the COMSOL Multiphysics environment. We examined 10-mm-wide cw LDBs mounted on a copper heat sink of the C–S mount type with FF = 50% and containing 47 emitting clusters. The following assumptions were made: uniform pumping of all the clusters in the bar over the entire range of pump currents studied, uniform thermal contact between all the clusters in the bar, constant thickness of the solder layer over the entire heat transfer area and zero LDB chip bend (smile). The boundary condition was the constant temperature (20 °C) of the lower face of the C–S mount.

For convenience of comparing simulation results and experimental data, we used the following parameter (‘thermal load’ of the laser chip):

$$P_{\text{therm}} = P_{\text{electr}}(1 - \eta_{\text{total}}), \quad (1)$$

where $P_{\text{electr}} = IV$ (I is the pump current and V is voltage) and η_{total} is the total efficiency. In the calculation, we used the experimentally determined output power ($L-I$ characteristic)

V.V. Bezotosnyi, V.P. Gordeev, V.A. Oleshchenko P.N. Lebedev Physical Institute, Russian Academy of Sciences, Leninsky prosp. 53, 119991 Moscow, Russia; e-mail: victorbe@sci.lebedev.ru

Received 26 March 2018; revision received 9 April 2018
Kvantovaya Elektronika 48 (6) 502–505 (2018)
Translated by O.M. Tsarev

and total efficiency as functions of pump current. Some of the data are presented in Fig. 1.

These data demonstrate that, at a pump current of 65 A and laser output power of 50 W, total efficiency is 40%, input electric power is $P_{\text{electr}} = 125$ W and, hence, the thermal load at this working point is $P_{\text{therm}} = 75$ W.

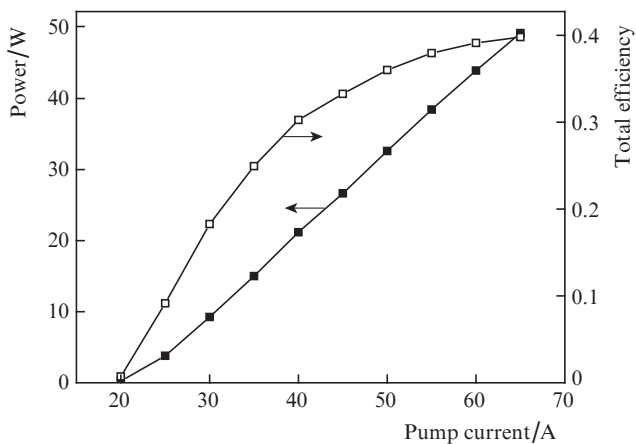


Figure 1. Output power and efficiency as functions of pump current for a laser diode bar.

Figure 2 presents 3D simulation results obtained in a thermal model for temperature profiles along a line across the active layer on the output mirror of the emitting aperture of a 47-cluster LDB at thermal loads from 10 to 100 W. The temperature profiles are modulated with a period corresponding to the spacing between the clusters. The modulation depth in the central clusters exceeds that in the peripheral clusters. With increasing thermal load, the modulation amplitude rises from a fraction of a degree Celsius at $P_{\text{therm}} = 10$ W to 2.5°C at 100 W. This is accompanied by an increase in the maximum temperature in the central cluster from 23 to 57°C. Thus, at a thermal load of 100 W, the overheating of the central cluster relative to the lower, thermally stabilised surface of the C–S mount (20°C) is 37°C. As expected,

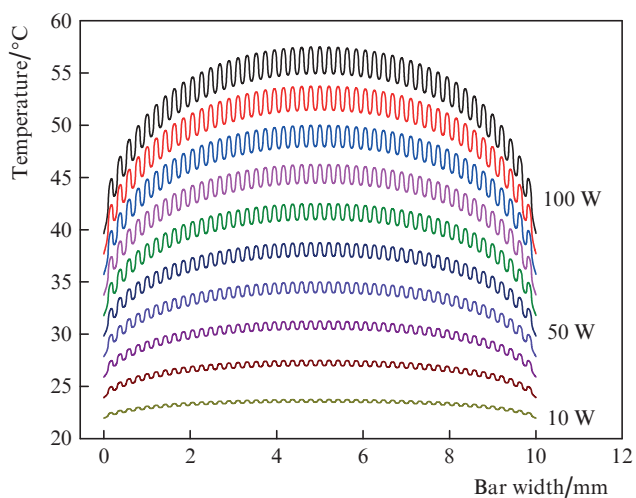


Figure 2. Temperature profiles along a line across the active region on the output mirror of an LDB at a thermal load varied from 10 to 100 W in 10-W steps.

increasing the number of clusters from 19 to 47 at constant FF and P_{therm} has little effect on the maximum temperature: at a thermal load of 60 W, the maximum temperature is 42.35°C for 19 clusters and 42.49°C for 47 clusters. The temperature difference is the result of slight changes in thermal flux in response to changes in cluster size.

3. Experimental results

To perform direct experimental verification of reliability of previously obtained results [3] and compare them to 3D simulation results, we measured temperature distributions over operating LDBs using a thermal camera. To improve its spatial resolution, we used a ZnSe lens, and to prevent stray lighting of the bolometer array with 808-nm light from the LDBs, we used a Si wafer polished on both sides. It is seen in the thermal camera image in Fig. 3 that the temperature under the central part of the LDB exceeds that under the peripheral clusters and that the temperature decreases towards the peripheral clusters and the lower face of the C–S mount. In spite of the measures taken to suppress stray lighting, the LDB output power in the measurements with the thermal camera was limited to a 10-W level in order to prevent damage to its optical components through heating by the LDB beam.

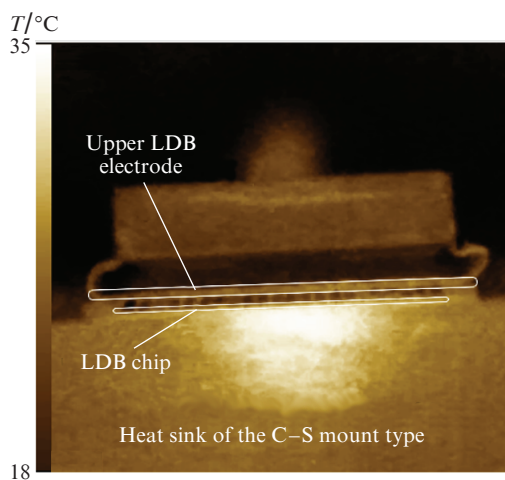


Figure 3. Thermal camera image of the front surface of an operating LDB at a thermal load of 45 W. The white contours indicate the position of the chip and upper LDB electrode.

To obtain adequate absolute temperatures, the thermal camera was calibrated. The image shown in Fig. 3 corresponds to a thermal load of about 50 W. The maximum temperature under the central part of the bar was 35°C and the basic temperature of the lower face of the C–S mount was 18°C (with a temperature difference of 17°C). The data in Fig. 2 show that, at this thermal load, the calculated temperature at the maximum of the distribution is 38°C at a basic temperature of 20°C, i.e. the temperature difference is 18°C, in good agreement with the thermal camera data.

Figure 4 shows a schematic of the experimental setup used to measure distributions of the power and emission spectrum over the aperture of cw LDBs. Samples of bars emitting at a wavelength of 808 nm were mounted on a C–S mount type heat sink. The packages of the C–S mounts of the LDBs were mounted on the massive block of a microchannel heat sink (Newport, USA) connected to a liquid cooling system. The

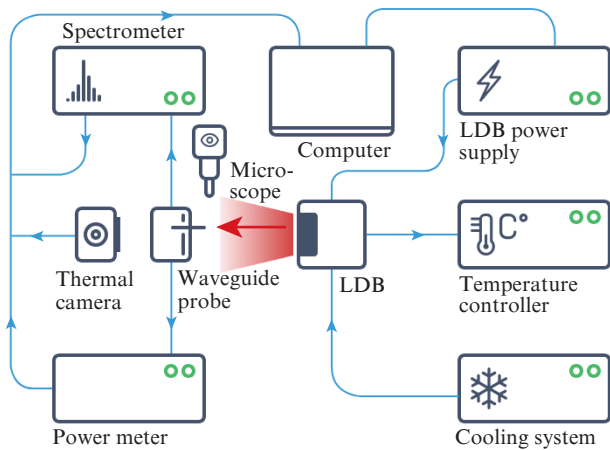


Figure 4. Experimental configuration.

bars were powered by a pump driver (Fedal, St. Petersburg) with a built-in pump control system. The integrated power of the LDB was measured using Gentec instruments (Canada). In contrast to previous work [3], the experimental configuration was refined with allowance for our previous measurement experience and requirements for measurements of parameters of LDBs with a large number of clusters. The measurements were automated using a motorised microtranslation stage (Standa, Lithuania) with a computer-controlled stepper motor. Mounted on the stage was a five-axis micrometer head (three coordinates and two angles) with a measuring probe. The head allowed for measurements on a series of LDBs with a large number of clusters. In addition, we modified the probe configuration: we designed and fabricated a two-channel probe for measuring the output power and emission spectrum. Its input aperture had a diameter of 250 μm . The configuration included a microscope, which allowed us to more accurately adjust and visually monitor the position of the input aperture of the probe relative to the LDB mirror while scanning the emitting aperture.

After a change in pump power, especially at a high thermal load, a certain time was needed for the LDB to reach a steady thermal state, so the output power and emission spectrum at each working point of the $L-I$ characteristic were measured after thermal equilibration. The data thus obtained were fed to a computer for further processing.

Figure 5 presents results obtained by scanning the output power over the LDB aperture at different pump currents. At a pump current of 25 A (Fig. 5a) and the corresponding output power near 4 W, the power profile is nonuniform, with a strong asymmetry on its left side. The lateral clusters are below the lasing threshold and the power distribution over the emitting part of the aperture has the form of quasi-periodic peaks with large dips. There is a modulation with a period corresponding to the spacing between the emitting clusters. At a pump current of 40 A (Fig. 5b) and output power of 21 W, the emitting aperture becomes markedly filled and lasing involves the lateral clusters. As a result, the envelope of the profile becomes even (but has a 50% dip in its centre); the power of the lateral clusters considerably rises, being only slightly (within 10%) below the average power; and a slight asymmetry persists on the left side. At a current of 55 A (Fig. 5c) and output power of 38 W, the profile is almost symmetric, the power in the lateral clusters approaches the average level of the distribution, and the power dip in the central clusters decreases from 50% to under 20%. On the whole, the picture of the filling of the LDB aperture with light with increasing pump current is qualitatively similar to that in broad stripe lasers.

Figure 6 shows calculated temperature profiles along the aperture of a 47-cluster LDB and typical experimental data extracted from spectral measurements by scanning the aperture (thermal load of 75 W). The vertical axis represents the temperature difference between the cluster being measured and the central (zeroth) cluster. The coinciding peaks of the calculated and experimental curves correspond to the position of the central cluster. There is good agreement in terms of temperature, but the experimental curve has a more complex shape. As distinct from the calculated curve, the experimental one is somewhat asymmetric, with three maxima: one at the centre of the LDB and the other two in symmetric positions 15 clusters away from the centre. It may be that this temperature profile reflects the thermoelastic stress distribution resulting from both the chip mounting process and the heating of the bar under operating conditions.

4. Discussion and conclusions

The temperature distribution along cw LDBs having an aperture width of 10 mm and containing 47 emitting clusters with FF = 50% has been studied using 3D simulation and

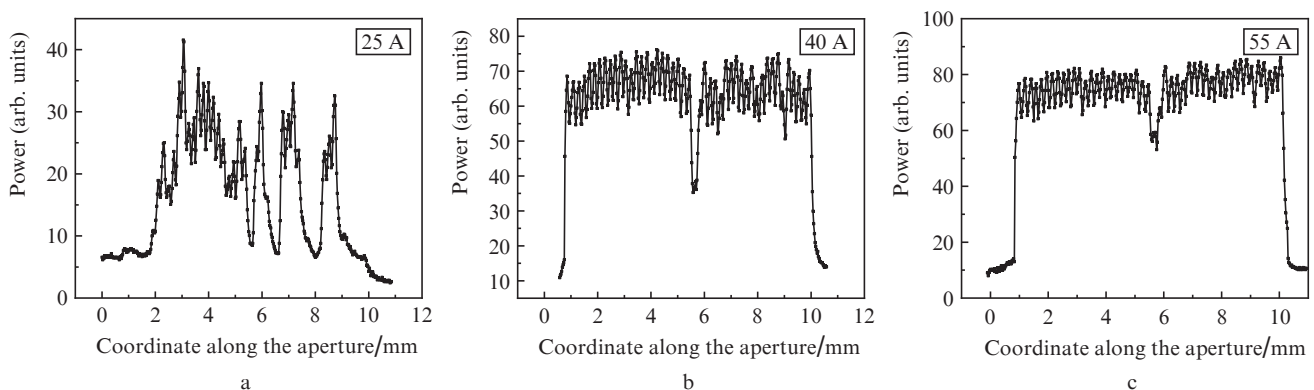


Figure 5. LDB output power profiles along the emission aperture at cw pump currents of (a) 25, (b) 40 and (c) 55 A.

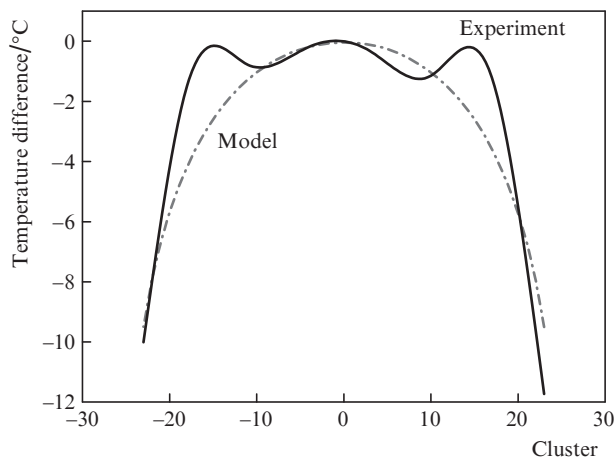


Figure 6. Calculated and experimentally determined temperature differences between the central (zeroth) cluster and peripheral clusters along the emitting aperture of an LDB at a thermal load of 75 W.

experimental measurements. We have calculated temperature profiles at different thermal loads. The temperature distributions measured in an operating LDB at relatively low output powers (thermal load under 50 W) using a thermal camera qualitatively confirm the nature of the temperature distribution and are well consistent with the temperature differences obtained by 3D thermal simulation at the corresponding thermal loads. We failed to measure temperature profiles at high laser output powers because of the stray lighting of the thermal camera and heating of the optical components by the LDB output.

The experimental setup has been modified for assessing the uniformity of the output power and emission spectrum of individual clusters. The output power distribution along the aperture of several LDBs has been measured at different pumping levels. The results demonstrate that raising the pump current reduces the difference in output power between individual clusters, ensures lasing in peripheral clusters, leads to a more complete filling of the aperture with light and reduces the asymmetry of the output power distribution. At an integrated output power of 38 W, the output power in the central part of the LDB is considerably lower (by up to 20%) than the average over all the clusters, which cannot be fully accounted for by the higher temperature in the centre due to the less favourable heat dissipation conditions because of the thermal effect of the peripheral clusters. Examination of the cluster cavity mirrors under a microscope at a high magnification detected no defects. The presence of bulk defects in the heterostructure of different LDB samples strictly in the central part of the laser chip appears unlikely. Further research is needed to resolve this issue. At the same time, examination of an enlarged near field at an output power above 60 W showed that the central part of the LDB had no narrow dips in power.

The temperature profiles extracted from spectral measurements by scanning the aperture agree well in magnitude with calculation results but have a more complex shape, which differs significantly from that of the calculated profile. This also requires further investigation.

The proposed measurement procedure, with the use of a probe, has an advantage over the scanning of an optically magnified near-field LDB image: it produces no distortions.

Such a procedure can be used for adjusting laser chip mounting process conditions and certifying and rapidly selecting LDBs according to the uniformity of the output power and spectrum of their emitting clusters, in particular for use in wavelength beam combining systems.

Acknowledgements. We are grateful to Yu.M. Popov, O.N. Krokhin, G.T. Mikaelyan and E.A. Cheshev for their assistance with and interest in this work and to N.G. Borisenko for providing the opportunity of utilising computational resources.

References

1. Bezotosnyi V.V., Kozyrev A.A., Kondakova N.S., Kondakov S.A., Krokhin O.N., Mikaelyan G.T., Oleshchenko V.A., Popov Yu.M., Cheshev E.A. *Kratk. Soobshch. Fiz.*, **12**, 41 (2016).
2. Bezotosnyi V.V., Kozyrev A.A., Kondakova N.S., Kondakov S.A., Krokhin O.N., Mikaelyan G.T., Oleshchenko V.A., Popov Yu.M., Cheshev E.A. *Quantum Electron.*, **47** (1), 5 (2017) [*Kvantovaya Elektron.*, **47** (1), 5 (2017)].
3. Bezotosnyi V.V., Gordeev V.P., Krokhin O.N., Mikaelyan G.T., Oleshchenko V.A., Pevtsov V.F., Popov Yu.M., Cheshev E.A. *Quantum Electron.*, **48** (2), 115 (2018) [*Kvantovaya Elektron.*, **48** (2), 115 (2018)].
4. Strohmaier S.G., Erbert G., Meissner-Schenk A.H., Lommel M., Schmidt B., Kaul T., Karow M., Crump P. *Proc. SPIE*, **10086**, 100860C-1 (2017).
5. Bezotosnyi V.V., Krokhin O.N., Oleshchenko V.A., Pevtsov V.F., Popov Yu.M., Cheshev E.A. *Quantum Electron.*, **44** (2), 145 (2014) [*Kvantovaya Elektron.*, **44** (2), 145 (2014)].
6. Crump P., Decker J., Winterfeldt M., Fricke J., Maaßdorf A., Erbert G., Tränkle G. *Proc. SPIE*, **9348**, 93480D-1 (2015).
7. Haas M., Rauch S., Nagel S., Beißwanger R., Dekorsy T., Zimer H. *IEEE J. Quantum Electron.*, **53** (3), 2600111 (2017).
8. Huang R.K., Chann B., Burgess J., Lochman B., Zhou W., Cruz M., Cook R., Dugmore D., Shattuck J., Tayebati P. *Proc. SPIE*, **9730**, 97300C-1 (2016).
9. Meng H., Ruan X., Du W., Wang Z., Lei F., Yu J., Ta H. *Laser Phys. Lett.*, **14**, 1 (2017).